ISSN: 2319-5967
ISO 9001:2008 Certified
International Journal of Engineering Science and Innovative Technology (IJESIT)
Volume 2, Issue 5, September 2013

Characterization of Cyclic Plastic Behavior of SS 316 Stainless Steel

J.Shit[a*], S.Dhar[b], S.Acharyya[b]
[a]Department of Mechanical Engineering, Raiganj Polytechnic, Uttar Dinajpur- 733134, India
[b]Department of Mechanical Engineering, Jadavpur University, Kolkata-700032, India

Abstract: ***This paper deals with experimental observation to characterize the cyclic plastic behavior of SS316 stainless steel. The cyclic plastic behavior includes symmetric strain controlled low cycle fatigue, cyclic hardening character of the material in transition cycles (from virgin state to saturated state) and uniaxial ratcheting phenomenon for non-symmetric stress controlled cyclic loading. The experimental data for strain controlled symmetric low cycle fatigue have been generated for first 30 cycles (beyond saturation) for different strain amplitudes. The ratcheting tests have been conducted for different ratcheting loads (various mean stresses and stress amplitudes). The ratcheting strain vs cycles data have been generated. Above all, tensile tests have been conducted to get mechanical properties of the material. Loop areas have been generated based on the cyclic elastic-plastic stress-strain response in order to identify the fatigue damage parameter. Fatigue strain life curves are generated for fatigue life prediction using Coffin- Manson and Basquin relation. The cyclic plastic stress-strain responses can be analyzed using the incremental plasticity theories and the results obtained from FE simulations can be compared with the experimental results at different strain amplitudes.***

Keywords: **Cyclic hardening, elastic-plastic, incremental plasticity, LCF, ratcheting.**

Nomenclature:

N = cycles to failure

$\Delta\varepsilon_p$ = plastic strain range

$\acute{\varepsilon}_f$ = fatigue ductility coefficient

$\Delta\varepsilon_e$ = elastic strain range

$\sigma_f^{'}$ = fatigue strength coefficient

b = fatigue strength exponent

$K^{/}$ = cyclic strength coefficient

$n^{/}$= cyclic strain hardening exponent

K= strength coefficient

n= hardening exponent

$\Delta\varepsilon$ = local strain range

$\Delta\varepsilon$ = total strain range considered

c = fatigue ductility exponent

ν= Poisson's ratio

E =Young's modulus

I. INTRODUCTION

SS316 is considered as the most preferred material for reactor structures and nuclear power plant components. Low cycle fatigue [1-3] must be considered during design of nuclear pressure vessels, steam turbines and other type of power machineries where life is nominally characterized as a function of the strain range and the component fails after a small number of cycles at a high stress, and the deformation is largely plastic. When the material is subjected to cyclic loading (e.g earthquake loading) i.e loading followed by unloading and subsequent reloading, the response change cycle by cycle until its gets saturated. Strain controlled cyclic loading is found in thermal cycling, where a component expands and contracts in response to fluctuations in the operating temperature or in reversed bending between fixed displacements. High temperature LCF tests on SS316 were investigated by Martin-Meizoso et al. [4] at temperature 600-625^{0}C. Experimental observation

ISSN: 2319-5967
ISO 9001:2008 Certified
International Journal of Engineering Science and Innovative Technology (IJESIT)
Volume 2, Issue 5, September 2013

shows that various cyclic plastic behavior [5-8] of the material. Those are i.) Bauschinger effect ii.) Cyclic hardening [9] iii.) Mean stress relaxation [8] and ratcheting [6-7, 10-12]. Some materials also show S-D (strength differential) effect [13]. Above all, there is additional hardening due to non proportional loading path. Xia and Ellyin [14] carried out biaxial tension/compression tests. Under non-proportional loading the stabilized response is independent of mean strain as in proportional loading case [15].

Ratcheting experiments have been conducted on different materials under various loading conditions by Hassan and Kyriakides [16], Hassan et al [17], Jiang and sehitoglu [18]. The cyclic hardening of metals tends to be stabilized after a certain number of cycles. Ratcheting, however, progresses with cycles even after stabilization. Generally piping systems in the nuclear power plant are designed for normal operating loads (pressure) along with cyclic loads. The cyclic loading on the piping with non-zero mean static stress results in either structural shakedown or ratcheting. With the occurrence of structural shakedown, the dissipated energy in the whole structure remains bounded after initial plastic flow and the structure responds in a purely elastic manner to the applied variable loads.

II. MATERIAL CHARACTERIZATION

A. Material

316 Stainless steel (SS316) is selected as material for the investigation. The chemical compositions of SS316 are shown in Table 1. Grade 316 is the standard molybde- num-bearing grade, second in importance to 304 amongst the austenitic stainless steels. Grade 316 L, the low car- bon version of 316 is immune from sensitisation (grain boundary carbide precipitation). Thus it is extensively used in heavy gauge welded components (over about 6 mm).

Table 1: Chemical composition of SS 316

Fe (%)	C (%)	Cr (%)	Ni (%)	Mo (%)	Mn (%)	Si (%)	P (%)	S (%)
-	<0.03	16-18.5	10-14	2-3	<2	<1	<0.045	<0.03

B. Material testing

1 Tensile test:

Cylindrical tensile specimens, made of SS316 steel are used for tensile test. The specimens are machined by taking coupons from longitudinal direction of the pipes. The diameter of the specimen is 6.5 mm and the gauge length is 30mm as shown in Fig.1. The tensile tests are performed at room temperature by using the servo hydraulic universal testing machine (Instron UTM) (Fig.2) with 100KN grip capacity, 8810 controller and data acquisition system. The testing process is computer controlled, where the Blue-hill software has been installed to control the testing process. The axial strain is measured by an extensometer of 12.5mm gauge length. This extensometer can measure up to 20% strain. The tensile test has been performed in displacement-controlled mode. The displacement rate is 0.5 mm\min. The tensile tests have been performed as per ASTM E8 standard. The data acquired in data acquisition system are processed to obtain the mechanical properties of the material. Those are listed in Table-4.1. Stress and plastic strain data obtained between the yield point and the ultimate point are used to generate a power law-hardening curve. The value of the strength coefficient '*K'* and hardening exponent '*n*' are also listed in Table-4.1 A stress-strain plot up to ultimate point is shown in Fig.3.

2 Low cycle fatigue tests:

Test materials was SS 316 stainless steel, which was solution treated at 1120°C for one hour and water quenched for 30 min. completely reversed strain controlled (Fig.4.) fatigue tests were performed to characterize the fatigue properties of the materials. Cylindrical specimen with diameter of 6.5mm and gauge length of 15 mm for plain fatigue (PF) is used as shown in Fig.5. A 100 KN servo-hydraulic Universal testing machine was used. A 12.5 gauge extensometer was attached to the specimens to measure the strain during the tests.

The strain-controlled tests were performed on the specimens for symmetric tension-compression strain cycles with the strain limits $\Delta\epsilon$= ±0.30%, ±0.50%, ±0.60%,± 0.75%,±1.00%, ±1.20%. During tests sinusoidal wave shape was used to control a constant strain rate of 10^{-2}/s.

ISSN: 2319-5967
ISO 9001:2008 Certified
International Journal of Engineering Science and Innovative Technology (IJESIT)
Volume 2, Issue 5, September 2013

3 Uniaxial ratcheting test:

The stress controlled ratcheting phenomenon is another aspect of low cycle fatigue responses. It is defined as the accumulation of plastic strain with cycles in the loading direction for non-symmetric stress controlled cyclic loading. The tests have been conducted in 100KN Instron UTM with 8810 controller and data acquisition system. The cylindrical fatigue specimen (Fig.5) with gauge length 15 mm and gauge diameter 6.5 mm is used for testing. The entire ratcheting test has been done under load-controlled mode. The loading history of the experiment is shown in Fig.6. Uniaxial ratcheting experiments are conducted at various combinations of mean stresses and stress amplitudes in this study. Thus the variation of mean stresses with constant stress amplitude and the variation of stress amplitudes with constant mean stress are taken in the test matrix. Those ratcheting loads are defined as m40a310, m60a310, m80a310, m80a270 and m80a350 respectively. The loading case m80a270 implies that the mean stress is 80 MPa and the stress amplitude is 270 MPa. A broad set of uniaxial ratcheting data of SS 316 steel has been generated from the experiment. These data can be used to evaluate the performance of the model. Fig.7 shows the uniaxial ratcheting response for the ratcheting load m80a350. The ratcheting strain variation with cycles under the condition of constant mean stress but varying amplitudes of stress is shown in Fig.8 (a) whereas Fig.8 (b) shows the variation of ratcheting strain with cycles under the situation of varying mean stresses with constant stress amplitude.

B. Experimental observations:

A cyclic strain symmetric test has been conducted in a 100 KN servo-hydraulic Universal testing machine (Fig.2) on a round tensile specimens for this material for different strain amplitude. Variation of tensile peak stress for different strain amplitude in a uniaxial cyclic test of and SS 316 stainless steel at strain rate of 10^{-2}/s at ambient temperature is shown in Fig.9.

Tensile peak stress with number of cycles for different strain amplitude is shown in Fig.9 and the following observations are made from the experiment for SS 316 stainless steel.

1. Hysteresis loops stabilize after about 30 cycles and the material arrives at an equilibrium condition for the imposed strain amplitude. Fig.10 shows experimental stress strain response up to 30^{th} cycles for strain amplitude 1.0%.

1. Strain amplitude 0.3% to 0.75% shows an initial hardening, a flat quasi- plateau for a large number of cycles and then softening before failure.
2. Strain amplitude 1.0% and 1.2% shows secondary hardening before failure. Also, it can be observed that cyclic hardening rate increase with strain amplitude.

Plasticity induced martensitic transformation of austenitic steel explains the secondary hardening as reported by Baudry et al.[19], Nebel[20] and Alain et al.[21].

Fig.11 shows the stabilized hysteresis loops between strees vs. true strain for different strain range of SS 316 stainless steel. Fig.12 shows the stabilized hysteresis loops between back strees vs. true plastic strain for different strain range of SS 316 stainless steel. The cyclic stress-strain curve is also shown in Fig.11 is obtained by connecting the positive peak of the stable hysteresis loops from constant strain amplitude fatigue tests of specimens cycled at different strain amplitude. The stabilized hysteresis loops are shifted in the way that the lower tips of the loops move to the origin as shown in Fig.14 and the non -massing behavior in which the upper branches do not coincide was observed. However the non-linear parts would coincide by translating each loop along the elastic portion as indicated in Fig.14.

The cyclic stress-strain curve shows higher hardening compared to the monotonic stress-strain curve as shown in Fig.13.

Cyclic stress-strain curve is expressed by a power curve as follows

$$\Delta\sigma = K^{/}\left(\Delta\varepsilon_p\right)^{n^{/}} \quad \text{.....(2.1)}$$

Where $K^{/}$ is cyclic strength coefficient and $n^{/}$ is the cyclic strain hardening exponent.

Equation (2.1) implies that the cyclic stress strain can be represented by a single straight line on a log-log plot, but since cyclic deformation behaviour may change appreciably with strain amplitude it is not unusual to find different slopes in the long life and short life fatigue regions.

ISSN: 2319-5967
ISO 9001:2008 Certified
International Journal of Engineering Science and Innovative Technology (IJESIT)
Volume 2, Issue 5, September 2013

Since $\frac{\Delta\varepsilon}{2} = \frac{\Delta\varepsilon_e}{2} + \frac{\Delta\varepsilon_p}{2}$

$$\frac{\Delta\varepsilon}{2} = \frac{\Delta\sigma}{2E} + \frac{1}{2}\left(\frac{\Delta\sigma}{K'}\right)^{\frac{1}{n'}} \quad \text{.....(2.2)}$$

This is the form of the equation for the cyclic stress strain curve.

Engineering approaches can face difficulty in the definition of cyclic stress strain curve for the materials which don't have the definite stabilized state such as given by the classical Ramberg Osgood equation [22].

And cyclic stress-strain curve is expressed by a power curve as follows

$$\frac{\Delta\sigma}{2} = K'\left(\frac{\Delta\varepsilon_p}{2}\right)^{n'} \quad \text{.....(2.3)}$$

Where K' is cyclic strength coefficient and n' is the cyclic strain hardening exponent.

$$\frac{\Delta\varepsilon}{2} = \frac{\Delta\varepsilon_e}{2} + \frac{\Delta\varepsilon_p}{2}$$

$$\Delta\varepsilon = \frac{\Delta\sigma}{E} + 2\left(\frac{\Delta\sigma}{2K'}\right)^{\frac{1}{n'}} \quad \text{.....(2.4)}$$

The dashed line in the Fig.15 is the predicted line with equation (2.4). The dashed line in the Fig.11 is the predicted line with equation (2.2).

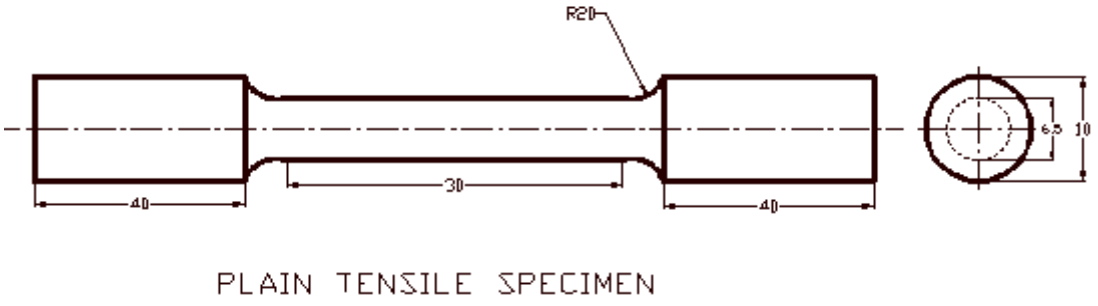

Fig.1: Uniaxial Tensile Specimen

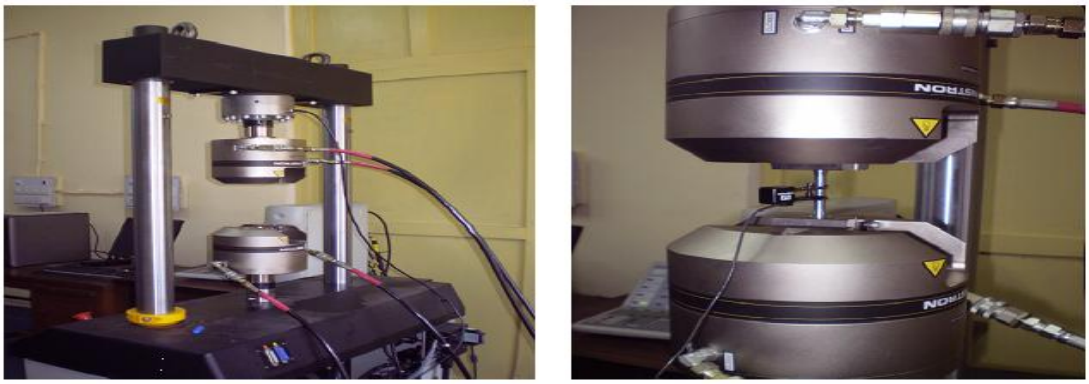

Fig.2: Experimental Equipment

ISSN: 2319-5967
ISO 9001:2008 Certified
International Journal of Engineering Science and Innovative Technology (IJESIT)
Volume 2, Issue 5, September 2013

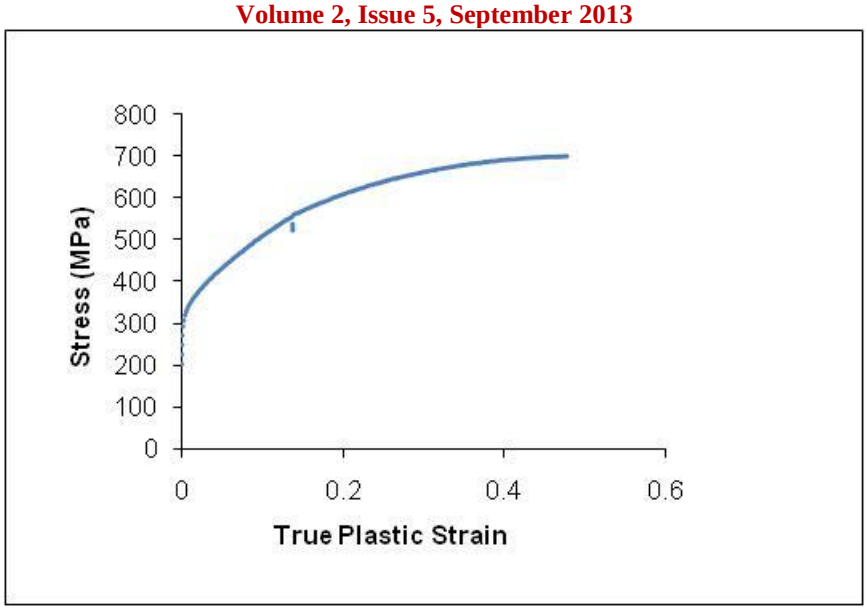

Fig.3: Stress-strain behavior of SS 316 steel.

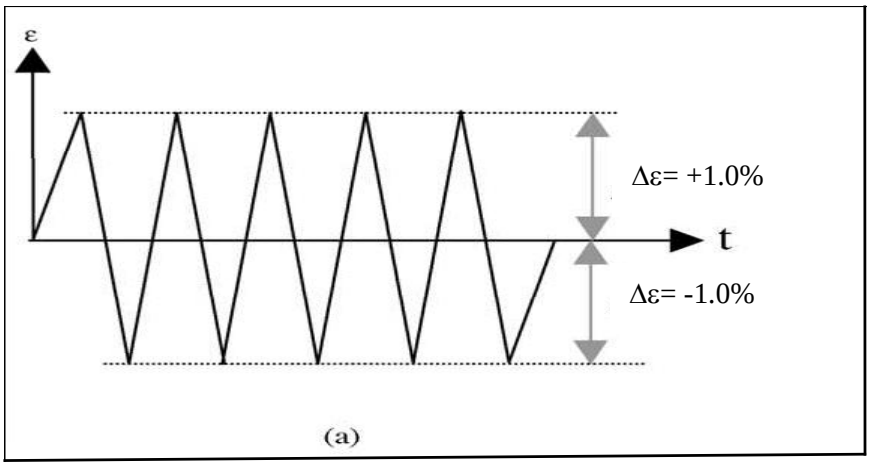

Fig.4: loading history during strain controlled test.

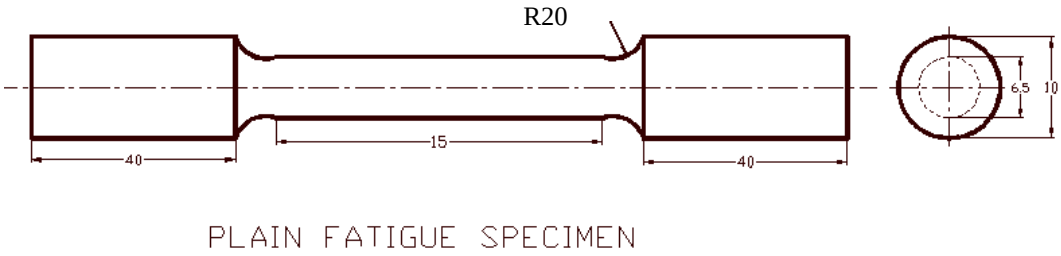

Fig.5: Uniaxial Fatigue Specimen.

ISSN: 2319-5967
ISO 9001:2008 Certified
International Journal of Engineering Science and Innovative Technology (IJESIT)
Volume 2, Issue 5, September 2013

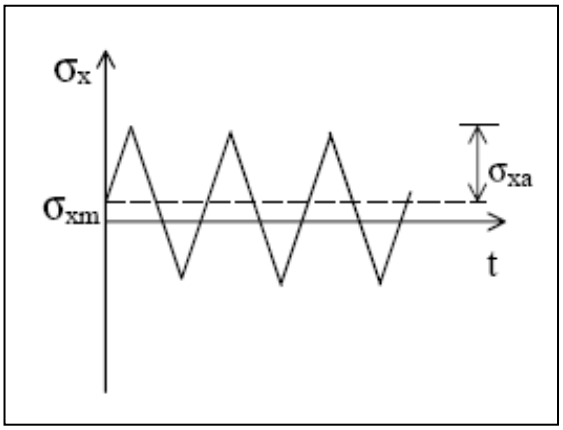

Fig.6: Loading histories; uniaxial stress cycles.

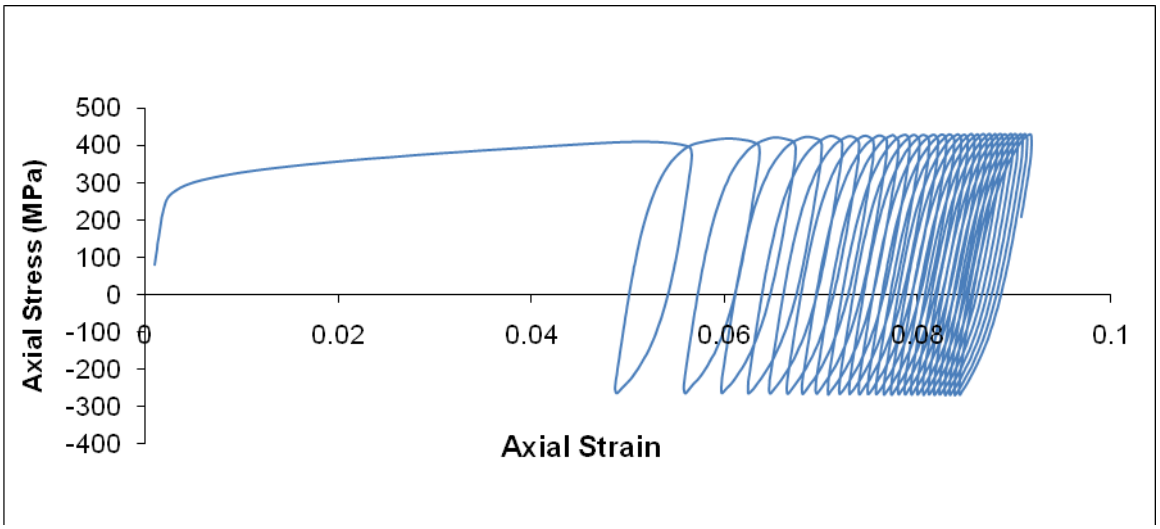

Fig.7: Axial ratcheting strain response for uniaxial stress controlled cycles with a mean stress (ratcheting load m80a350).

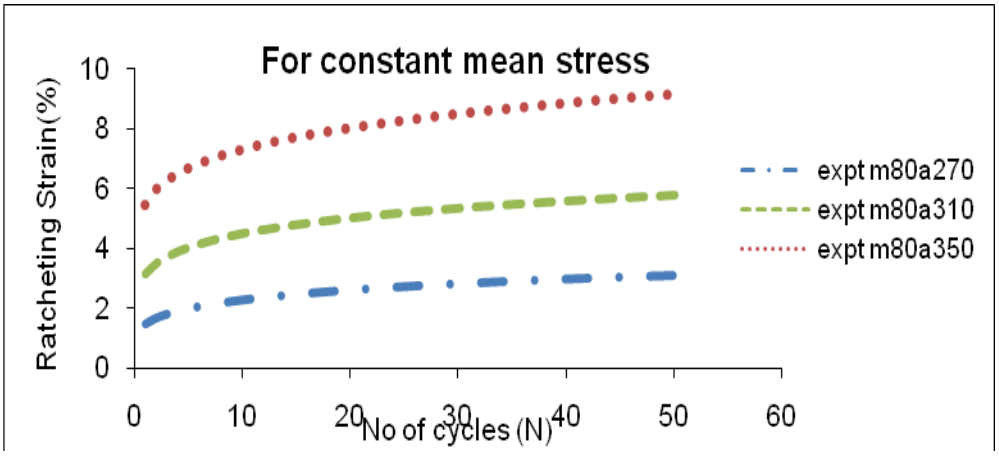

ISSN: 2319-5967
ISO 9001:2008 Certified
International Journal of Engineering Science and Innovative Technology (IJESIT)
Volume 2, Issue 5, September 2013

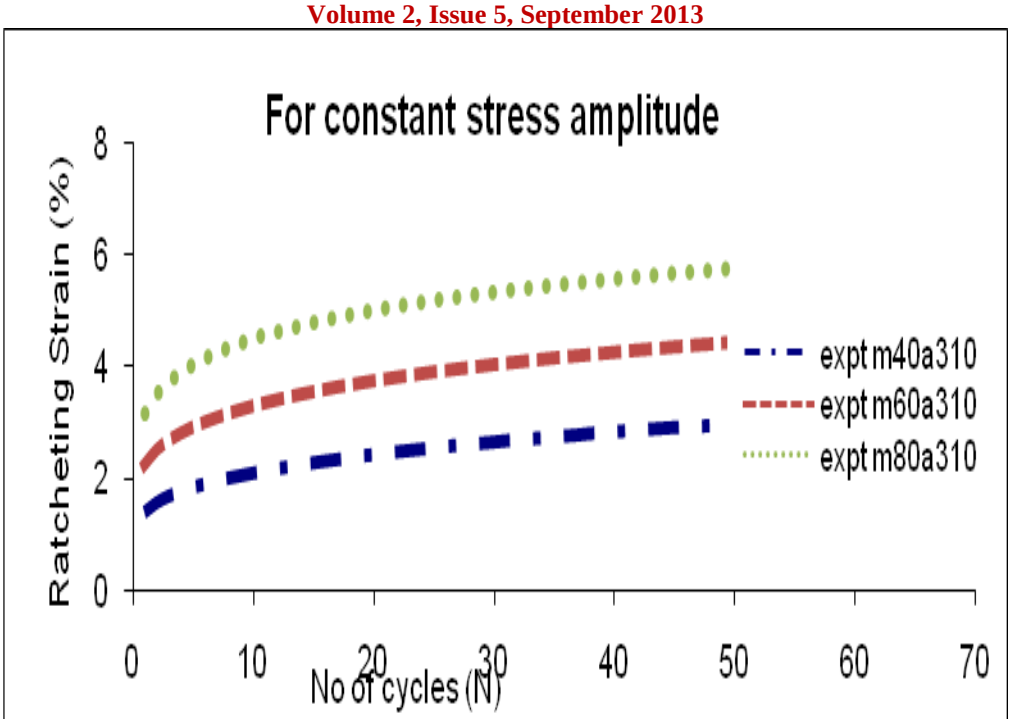

Fig.8: (a) Experimental ratcheting strain vs. cycle for constant mean stress. (b) Experimental ratcheting strain vs. cycle for constant stress amplitude.

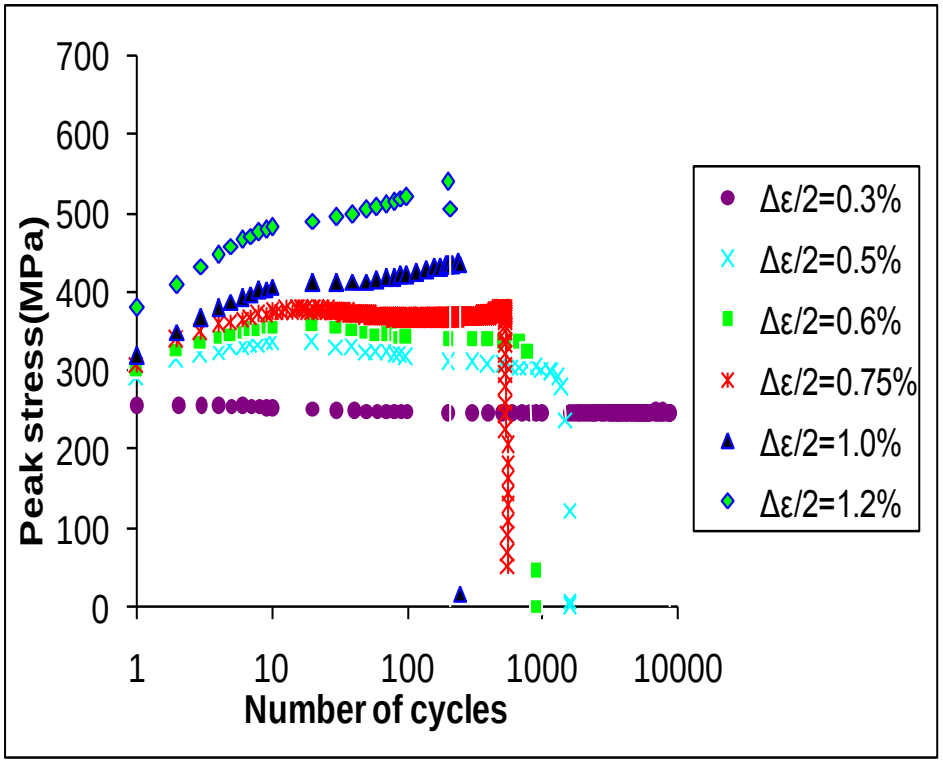

Fig.9: Tensile peak stress vs. number of cycles.

ISSN: 2319-5967
ISO 9001:2008 Certified
International Journal of Engineering Science and Innovative Technology (IJESIT)
Volume 2, Issue 5, September 2013

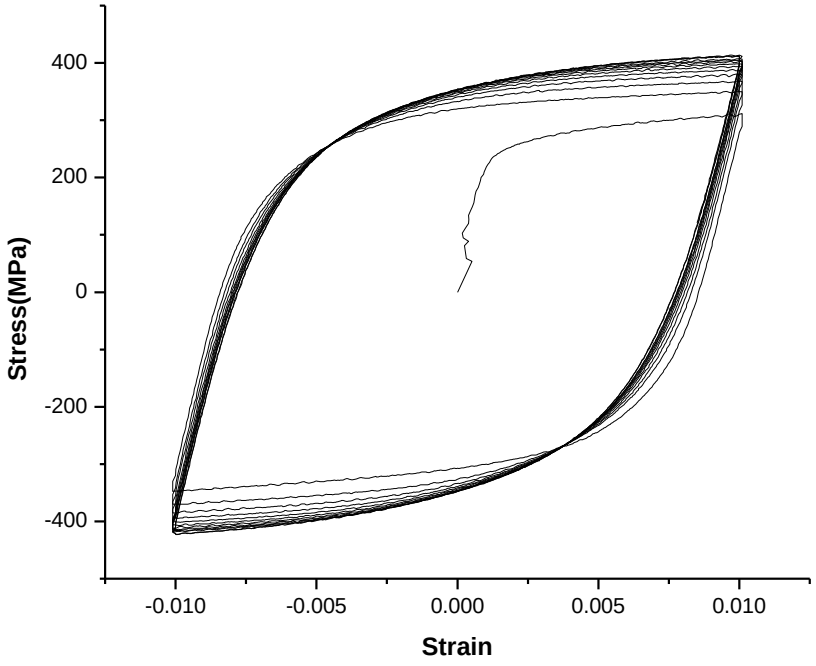

Fig.10: Experimental stress strain response up to 30th cycles for 1% strain amplitude curve.

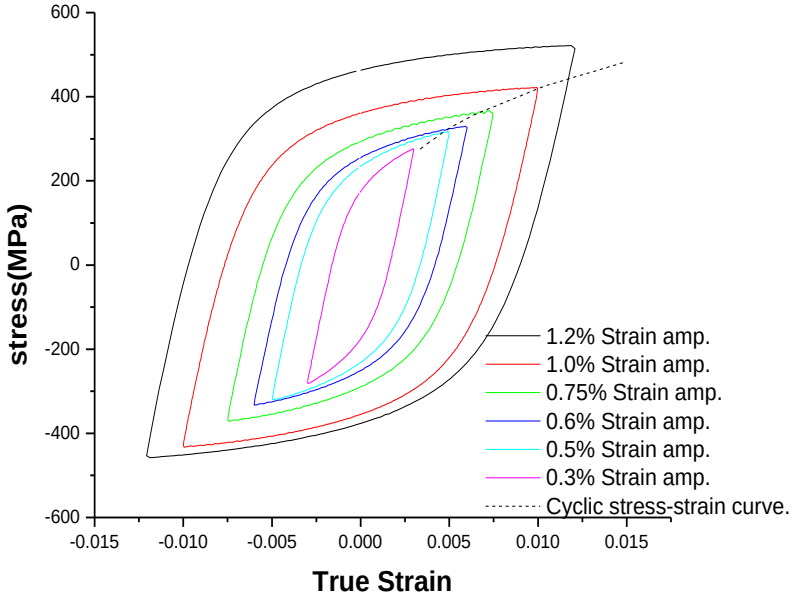

Fig.11: stabilized hysteresis loops between Stresses vs. True strain for different strain range.

ISSN: 2319-5967
ISO 9001:2008 Certified
International Journal of Engineering Science and Innovative Technology (IJESIT)
Volume 2, Issue 5, September 2013

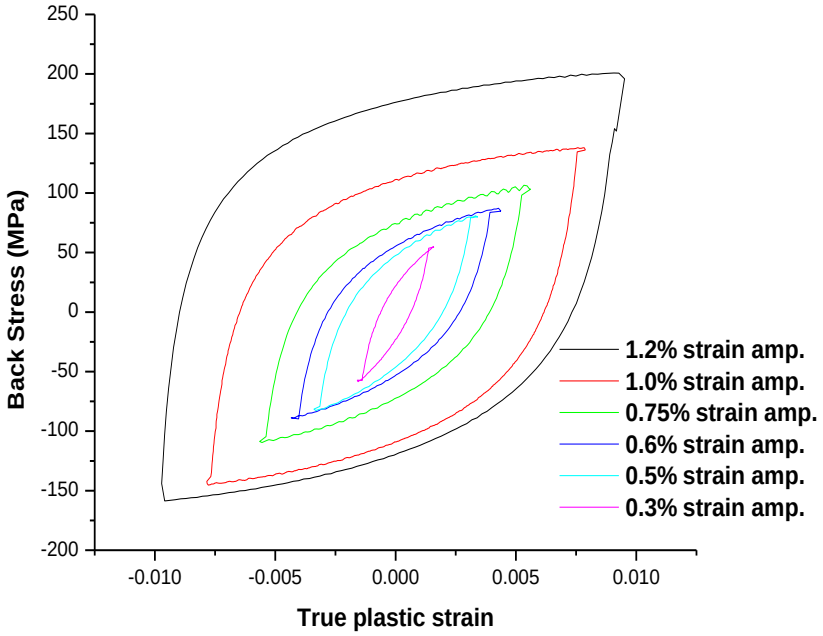

Fig.12: stabilized hysteresis loops between Back stress vs. True plastic strain for different strain range.

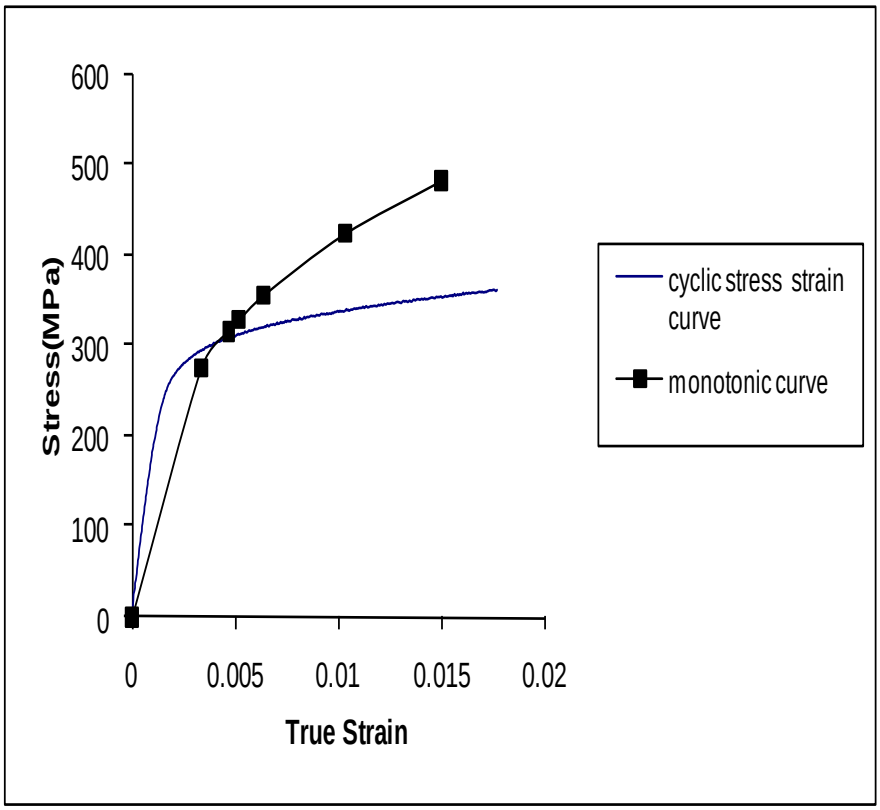

Fig.13: The cyclic stress strain curve as compared with the monotonic curve.

ISSN: 2319-5967
ISO 9001:2008 Certified
International Journal of Engineering Science and Innovative Technology (IJESIT)
Volume 2, Issue 5, September 2013

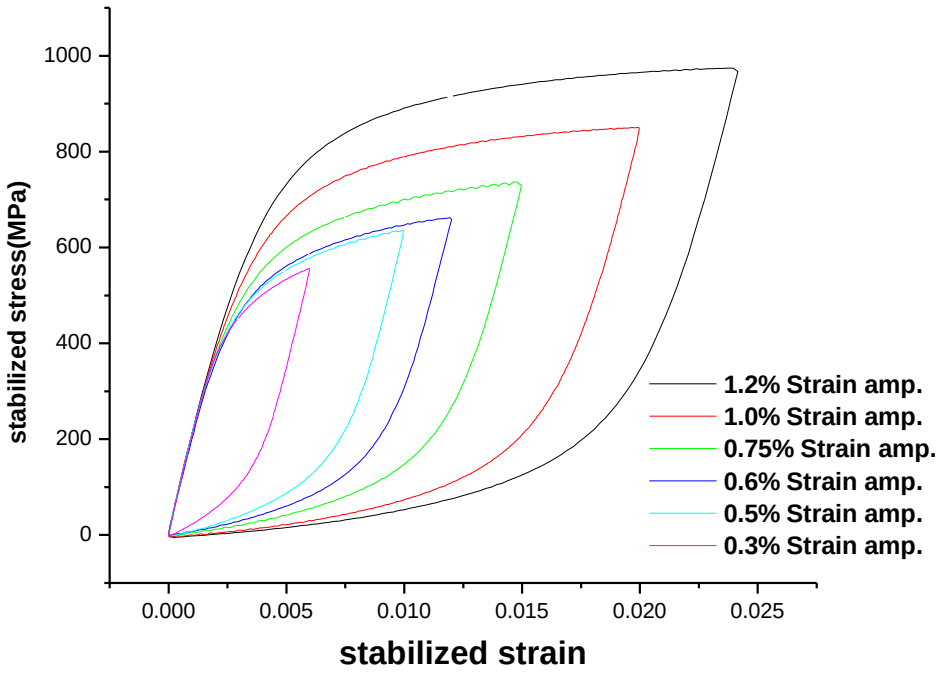

Fig.14: Stabilized hysteresis loops shifted to the origin.

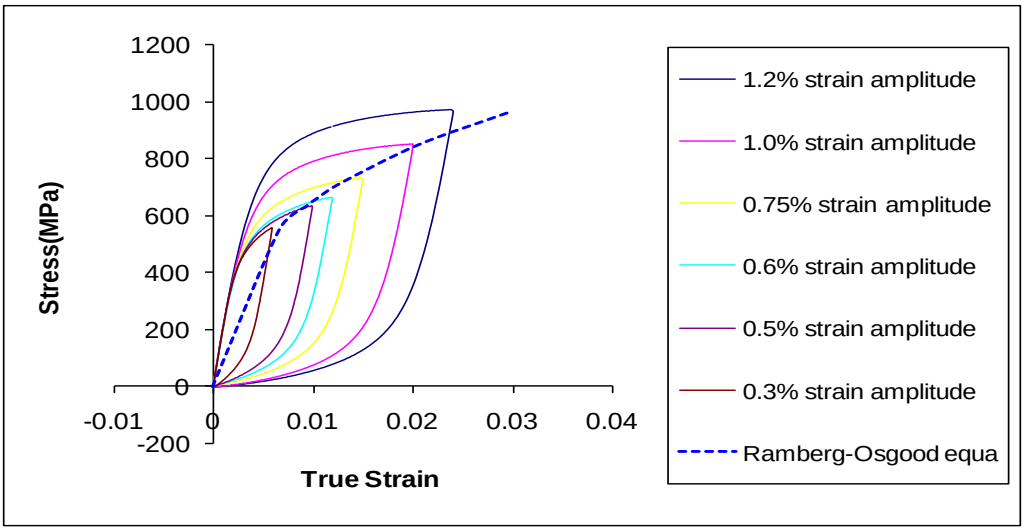

Fig.15: Stabilized hysteresis loops shifted to the origin showing Ramberg-Osgood equation.

Mean Stress Relaxation:

Relaxation of mean stress happens when we do an unsymmetrical strain cycling. For unsymmetrical strain controlled experiment, a mean strain is introduced. Mean strain cause mean stress. So at the initial cycle a mean stress is introduced during unsymmetrical strain controlled experiment. But as the cycling proceeds mean stress will relax and tends to zero. The nonlinear kinematic hardening model is capable of addressing this behavior. The specimen is cycled between 1.5% (Plastic strain) to 1.8% (Plastic strain) with a mean strain of 1.65% (Plastic strain). The mean stress relaxation is achieved in this model shown in Fig.15.

ISSN: 2319-5967
ISO 9001:2008 Certified
International Journal of Engineering Science and Innovative Technology (IJESIT)
Volume 2, Issue 5, September 2013

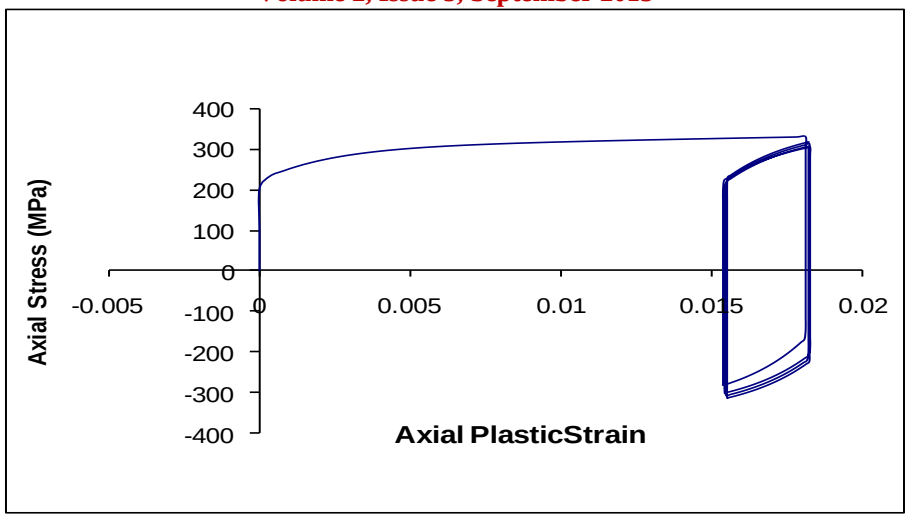

Fig.16: Mean stress relaxation for the plastic strain amplitude ± 0.15%.

III. LOW CYCLE FATIGUE (LCF) OR STRAIN BASED FATIGUE

Fatigue failure under Low-cycle fatigue is usually characterized by Plastic strain –life relation known as *Coffin-Manson relation*, which is best described by

$$\frac{\Delta\varepsilon_p}{2} = \varepsilon_f^{/}(2N)^C \quad \text{.....(3.1)}$$

Where ,

- $\frac{\Delta\varepsilon_p}{2}$ = plastic strain amplitude
- $\acute{\varepsilon}_f$ = fatigue ductility coefficient defined by the strain intercept at 2N = 1. $\acute{\varepsilon}_f$ is approximately equal to the true fracture strain ε_f for many metals.
- 2N = number of strain reversal to failure (1 cycle = 2 reversals)
- c = fatigue ductility exponent (for many metals c varies between 0.5 and – 0.7).

A smaller value of c results in larger values of fatigue life. Morrow [23] has shown that c = -1/(1+5ń), so that materials with larger values of ń have longer fatigue lives.

Table- 2: Plane fatigue test data from experiment:

Strain amp (%)	Peak plastic strain at saturation	Failure at (cycles)
1.2	0.0095	210
1.0	0.0078	247
0.75	0.0056	562
0.6	0.00437769	1224
0.5	0.0034	1602

Using plain fatigue test data the above constants are determined and the values are C=-0.4503 and $\varepsilon_f^{/}$ =0.1357.

ELASTIC STRAIN FATIGUE LIFE CURVE

The relation between elastic strain and fatigue life in the high cycle fatigue can be described by the Basquin's reformulated equation. Basquin's reformulated equation is best described by

$$\sigma_a = (\Delta\varepsilon_e/2)\, E = \sigma'_f (2N)^b \quad \text{.....(3.2)}$$

ISSN: 2319-5967
ISO 9001:2008 Certified
International Journal of Engineering Science and Innovative Technology (IJESIT)
Volume 2, Issue 5, September 2013

$\Delta\varepsilon_e/2=$ elastic component of the cyclic strain amplitude

E=Young's modulus.

σ_a = cyclic stress amplitude

σ'_f=fatigue coefficient defined by the stress intercept at 2N=1. σ'f is approximately equal to the monotonic true fracture stress,σ_f.

N = cycles to failure

b = fatigue strength exponent.

Table- 3: Plane fatigue test data from experiment:

Strain amp (%)	Peak elastic strain at saturation	Failure at (cycles)
1.2	0.0025	210
1.0	0.0022	247
0.75	0.00188	562
0.6	0.0016223	1224
0.5	0.00159	1602

Using plain fatigue test data the above constants are determined and the values are

b= -0.209, $\frac{\sigma_f'}{E}=0.00839$

Summing the elastic and plastic components can form the Strain-Life Curve:

$$\frac{\Delta\varepsilon}{2}=\frac{\Delta\varepsilon_e}{2}+\frac{\Delta\varepsilon_p}{2}$$

$$\frac{\Delta\varepsilon}{2}=\frac{\sigma_f'}{E}(2N)^b+\varepsilon_f'(2N)^C \quad \text{.....(3.3)}$$

The above equation is valid for the entire range of fatigue life, is obtained by superposition of elastic and plastic strain and the plot of 2N (reversals to failure) vs total strain amplitude is shown below.

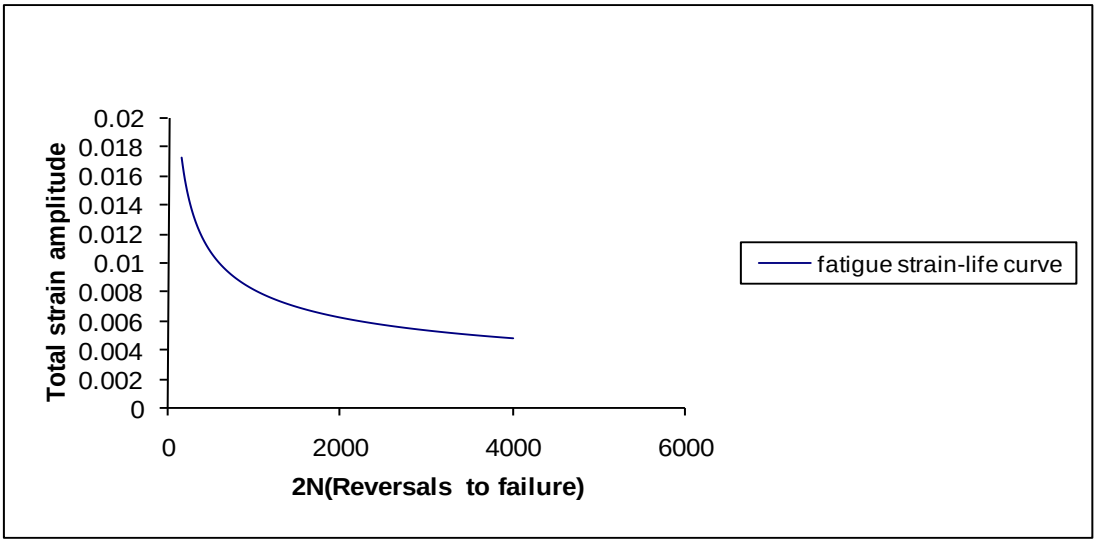

Fig.17: Fatigue strain-life curve.

ISSN: 2319-5967
ISO 9001:2008 Certified
International Journal of Engineering Science and Innovative Technology (IJESIT)
Volume 2, Issue 5, September 2013

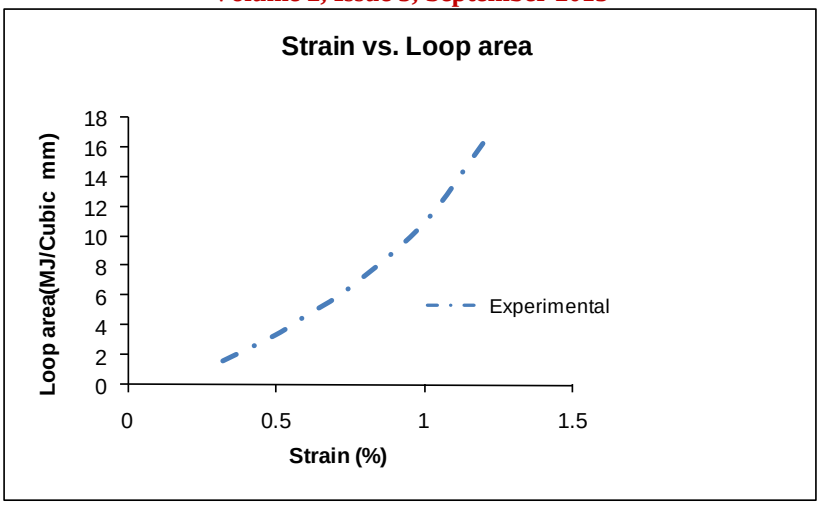

Fig.18: Loop area (between stress vs. strain) vs. strain curve.

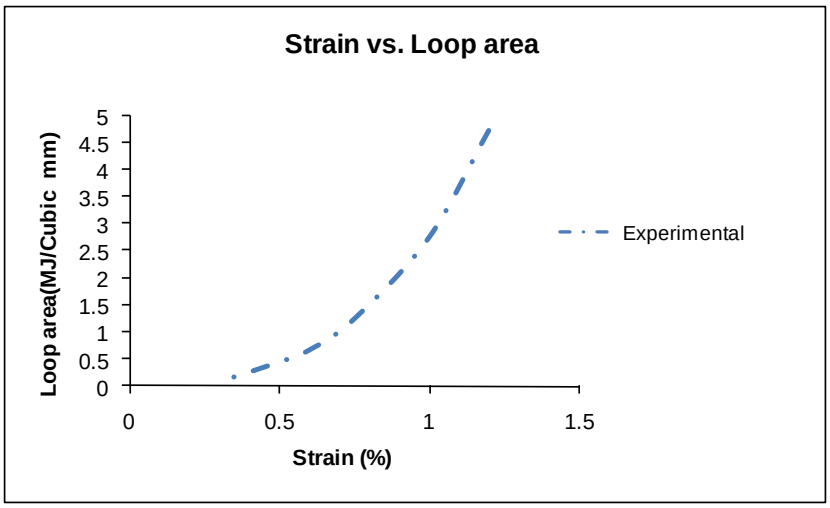

Fig.19: Loop area (between back stress vs. plastic strain) vs. strain curve.

IV. MECHANICAL PROPERTIES OF SS316

Table-4. Tensile Properties:

Young's Modulus (GPa)	Poisson's Ratio	σ_{YP} (MPa)	σ_{UTS} (MPa)	% Elongation	$\sigma=K(\varepsilon_p)^n$	
					K	n
210	0.3	267	637	78	1150	0.286

Table-5: Variation of cyclic yield stress with strain amplitudes

ε_p(%)	$(\sigma_{YP})_{cyc}$ (MPa)
0.81	215
0.43	199
0.33	196

ISSN: 2319-5967
ISO 9001:2008 Certified
International Journal of Engineering Science and Innovative Technology (IJESIT)
Volume 2, Issue 5, September 2013

V. DISCUSSION & CONCLUSIONS

The present work is an attempt for characterization of experimental observation of various cyclic plastic behavior of SS316. Those are i.) Bauschinger effect ii.) Cyclic hardening iii.) Mean stress relaxation and ratcheting. The experiments are performed at room temperature by using the servo hydraulic universal testing machine (Instron UTM) with 100 KN grip capacity, 8810 controller and data acquisition system. The testing process is computer controlled, where the Blue Hill and SAX software has been installed to control the testing process. Strain controlled test were performed on the specimens at different strain amplitudes. Cyclic hardening is observed from the experimental loops, which saturates after about 30 cycles. Most of the curves ($\in_a$=0.3%-0.75%) show initial hardening, flat region for a large no. of cycles and then softening. Secondary hardening is observed for strain amplitude $\in_a$=1.0% and 1.20% respectively. Ratcheting strain i.e accumulation of large plastic strain in the loading direction for nonsymmetrical (non zero mean stress) stress controlled cyclic loading is also observed. Ratcheting strain increases with the increase of mean stress and stress amplitude. For each ratcheting load it is observed that rate of ratcheting decreases with cycle and subsequently gets stabilized. The loop areas for various strain amplitudes are calculated. Fatigue strain life curves, as shown in Fig.17 are generated for fatigue life prediction at different strain range using Coffin- Manson and Basquin relation. Fig.18 shows Loop area (between stress vs. strain) vs. strain curve and Fig.19 shows Loop area (between back stress vs. plastic strain) vs. strain curve. Loop areas have been generated based on the cyclic elastic-plastic stress-strain response in order to identify the fatigue damage parameter. Fatigue strain life curves are generated for fatigue life prediction for different strain range as in LCF life is nominally characterized as a function of the strain range. Ratcheting is important in designing and the life evaluation of the structural components endured in cyclic loading as in design and analysis of structure ratcheting can lead to catastrophic failure of the structures and the phenomenon culminates to either plastic shake down or to a rapid increase in ratcheting strain leading to failure. Above all the experimental data are very useful for calibration purpose during simulation.

REFERENCES

[1]. Lim Jae-Yong, Hong Seong-Gu, Lee Soon-Bok. Application of local stress-strain approaches in the prediction of fatigue crack initiation life for cyclically non stabilized and non-masing steel. International journal of fatigue 27 (2005) 1653-1660.

[2]. Dutta A, Dhar S, Acharyya S.K. Material characterization of SS 316 in low cycle fatigue loading. J Mater Sci (2010) 45: 1782-1789.

[3]. Shit J, Dhar S, Acharyya S. Modeling and Finite Element Simulation of Low Cycle Fatigue Behavior of 316 SS. 6th International Conference on Creep, Fatigue and Creep-Fatigue Interaction [CF-6]. Procedia Engineering 55 (2013) 774–779.

[4]. Martin-Meizoso A, Rodriguez-Ibabe JM, Fuentes-Perez M (1993) Int J Fract 64:R45

[5] Paul Surajit Kumar, Sivaprasad S, Dhar S, Tarafder M, Tarafdaer S. Simulation of cyclic plastic deformation response in SA 333 C-Mn steel by a kinematic hardening model. Computational material science 48 (2010) 662-671.

[6]. Hassan Tasnim, Kyriakides Stelios. Ratcheting in Cyclic Plasticity, Part I: Uniaxial Behavior. International journal of plasticity, vol 8, pp. 91-116, 1992.

[7] Hassan Tasnim,Corona Edmundo, and Kyriakides Stelios. Ratcheting in Cyclic Plasticity, Part II: Multiaxial Behavior. International journal of plasticity, vol 8, pp. 117-146, 1992.

[8] Shit J, Dhar S, Acharyya S. Experimental and numerical simulation of carbon manganese steel for cyclic plastic behavior. International Journal of Engineering, Science and Technology Vol. 2, No. 4, 2010, pp. 71-84.

[9]. Kang Guozheng, Ohno Nobutada, Nebu Akira. Constitutive modeling of strain range dependent cyclic hardening. International journal of plasticity 19 (2003) 1801-1819.

[10]. Kulkarni S.C, Desai Y.M, Kant T, Reddy G.R, Prasad P, Vaze K.K, Gupta C. International journal of Pressure Vessels and Piping 81 (2004) 609-617.

[11]. Hassan Tasnim, Kyriakides Stelios. Ratcheting of cyclic hardening and softening materials: I. Uniaxial Behavior. International journal of plasticity, vol 10, pp. 149-184, 1994.

[12]. Shit J , Dhar S, Acharyya S. K, Goyal S. Modeling of uniaxial ratcheting behavior of SA333 carbon manganese steel. International Journal of Pressure Vessels and Piping 92 (2012) 96-105.

ISSN: 2319-5967
ISO 9001:2008 Certified
International Journal of Engineering Science and Innovative Technology (IJESIT)
Volume 2, Issue 5, September 2013

[13]. Chaboche J.L, Dang Van, Cordier G. 'Modelization of the Strain Memory Effect on Cyclic Hardening of 316 Stainless Steel'. Paper L 11/3 1979; 5th SMIRT, Berlin.

[14]. Ellyin F, Xia Z. 'A Rate Independent Constitutive Model for Transient Non Proportional Loading'. JL. Mech. Phys. Solids 1989; 37: 71.

[15]. Benallal A, LeFallo P, Marquis D. 'An Experimental Investigation of Cyclic Hardening of 316 Stainless steel and 2024 Aluminum Alloy under Multiaxial Loading'. Nucl. Engg. Des 1989; 114:345.

[16]. Hassan .T, Kyriakids .S (1992). 'Racheting in cyclic plasticity, Part I, uniaxial behavior'. Int. Jl. Plasticity, 8, 91-116.

[17]. Hassan .T, Corona E, Kyriakids .S (1992). 'Racheting in cyclic plasticity, Part II, multiaxial behavior'. Int. Jl. Plasticity, 8, 117-145.

[18]. Jiang.Y.Y , Sehitoglu (1994) . 'Cyclic ratcheting of 1070 steel under multiaxial stress state'. Int. Jl. Plasticity, 10, 579-608.

[19] Baudry G, Pineau A. influence of strain induced martensitic transformation on the low-cycle fatigue behavior of a stainless steel. Mater Sci Eng A 1977; 28:229-42.

[20] Nebel Th, Difler D. cyclic deformation behavior of austenitic steels at ambient and elevated temperatures. Sadhana 2003; 28 (1-2): 187-208.

[21] Alain R, Violan P, Mendez J. low cycle fatigue behavior in vacuum of a 316L type austenitic stainless steel between 20 and 600^0c part I: fatigue resistance and cyclic behavior. Mater Sci Eng A 1997; 229:87-94.

[22] Ramberg W, Osgood WmR.Description of stress-strain curves by three parameters, NACA TN-902. Washington, DC: National Advisory committee for Aeronautics; 1943.

[23] J.D.Morrow, in "International Friction, Damping and cyclic Plasticity," ASTM.STP No. 378, p. 72, ASTM, Philadelphia, 1965.

AUTHOR BIOGRAPHY

Dr. Jagabandhu Shit is a Lecturer in Raiganj Polytechnic College, West Bengal. He is engaged in teaching and research activities since the last 5 years. His field of specialization is Plasticity. He is doing his research work in the area of LCF and ratcheting. He has published several papers in various national, international conferences and journals. He has completed his PG from Mechanical Engineering Department Jadavpur University.

Dr. Sankar Dhar is a Professor of Mechanical Engineering, Jadavpur University (India). He is engaged in teaching and research activities since the last 25 years. His field of specialization is Plasticity and Ductile fracture. Dr. Dhar has a lot of experience in supervising several projects from BARC and DRDO. He worked in CEA, France for two years. He has published several papers in various national, international conferences and journals. He has guided 3 students for their Ph.D.work.

Dr. Sanjib Acharyya is working as a Reader in Mechanical Engineering Department, Jadavpur University, India. He is engaged in teaching and research activities since the last 18 years. His field of specializations is Ductile fracture and Material Characterization and Design Optimization. Dr. Acharyya has been supervising several projects from BARC and DRDO. He has published several papers in various national, international conferences and journals. At present he is guiding 4 students for their Ph.D. work.